



Science Arts & Métiers (SAM)

is an open access repository that collects the work of Arts et Métiers Institute of Technology researchers and makes it freely available over the web where possible.

This is an author-deposited version published in: <https://sam.ensam.eu>
Handle ID: <http://hdl.handle.net/10985/24731>

To cite this version :

Komi Franck GBEKOU, Abderrahim BOUDENNE, Anissa EDDHAHAK, Karim BENZARTI - Mechanical and thermal properties of cement mortar composites incorporating micronized miscanthus fibers - Journal of Materials Research and Technology - 2023

Any correspondence concerning this service should be sent to the repository

Administrator : scienceouverte@ensam.eu





Available online at www.sciencedirect.com
jmr&t
 Journal of Materials Research and Technology
 journal homepage: www.elsevier.com/locate/jmrt



Mechanical and thermal properties of cement mortar composites incorporating micronized miscanthus fibers

Franck Komi Gbekou ^a, Abderrahim Boudenne ^b, Anissa Eddhahak ^c,
 Karim Benzarti ^{a,*}

^a Univ Gustave Eiffel, Ecole des Ponts, CNRS, Navier, F-77447 Marne-la-Vallée, France

^b Univ Paris-Est Créteil, CERTES, F-94010 Créteil, France

^c Arts et Métiers ParisTech, Laboratoire Procédés et Ingénierie en Mécanique et Matériaux (PIMM), F-75013 Paris, France

ARTICLE INFO

Article history:

Received 6 June 2023

Accepted 11 September 2023

Available online 13 September 2023

Keywords:

Bio-based mortar

Miscanthus fibers

Micronized powder

Thermal and mechanical characteristics

Microstructural characterization

ABSTRACT

This study examines the impact of incorporating micronized miscanthus fibers into a cement mortar, focusing on the mechanical and thermal effects. Initially, an experimental procedure was devised to create mortar mixtures with varying amounts of miscanthus fibers, with a maximum dosage of 7 wt%. This involved saturating the fibers with water beforehand to maintain the workability of the fresh mixes. The resulting hardened bio-based mortars were then evaluated after 28 days in terms of their microstructure, mechanical strength (assessed through flexural and compression tests), and thermophysical properties (measured using the Hot-Disk technique to determine thermal conductivity/diffusivity and volumetric heat capacity). The experimental findings revealed significant enhancements (up to 87%) in the thermal resistance of the mortars due to the addition of fibers. However, this improvement was accompanied by a considerable reduction in mechanical strength. As a result, while these bio-based mortars are unsuitable for structural applications, they still possess adequate mechanical properties for handling and are appropriate for insulation purposes in construction.

© 2023 The Author(s). Published by Elsevier B.V. This is an open access article under the CC BY license (<http://creativecommons.org/licenses/by/4.0/>).

1. Introduction

In recent decades, the buildings and construction sector has witnessed a significant surge in the consumption of fossil energy, leading to a substantial rise in CO₂ emissions. Economic expansion and the increase in population are the primary factors behind this trend, which leads to depletion of

natural resources and harm to the environment [1]. To address this issue, public initiatives foster the development of cutting-edge technologies aimed at enhancing energy efficiency, with a particular emphasis on eco-friendly solutions.

From this perspective, the substitution of traditional building materials with bio-based alternatives showing low thermal conductivity (or high thermal resistance) has become an attractive way for improving the thermal efficiency and

* Corresponding author.

E-mail addresses: komi.gbekou@univ-eiffel.fr (F.K. Gbekou), boudenne@u-pec.fr (A. Boudenne), Anissa.EDDHAK@ensam.eu (A. Eddhahak), karim.benzarti@univ-eiffel.fr (K. Benzarti).

<https://doi.org/10.1016/j.jmrt.2023.09.093>

2238-7854/© 2023 The Author(s). Published by Elsevier B.V. This is an open access article under the CC BY license (<http://creativecommons.org/licenses/by/4.0/>).

decreasing the carbon impact of buildings [2,3]. Moreover, these bio-based materials tend to have hygroscopic properties, allowing them to absorb or release moisture, thus reducing indoor air humidity fluctuations. This not only makes them effective as thermal insulation, but also contributes to a healthier and more comfortable living environment. Among these new materials, the development of bio-based concrete has taken an important place [2,4]. It consists in mixing agricultural by-products or wastes with mineral binders (for instance cement mortars, gypsum, earth, etc ...) to design novel building materials. Such plant-based products offer an environmentally friendly and renewable option as they are selected based on sustainability factors like local availability and cost of processing.

Extensive research has been conducted on the utilization of various plant fibers such as hemp, flax, wood, cork, rice husk, straw, and date palm fibers [5–13]. Thanks to their lightweight and highly microporous structure, these fibers have been successfully used to develop ultra-lightweight concrete suitable for building insulation. The majority of these studies have indicated that incorporating plant fibers into cement materials yields improved thermal performance, notably through a significant reduction in thermal conductivity. Additionally, the inclusion of plant fibers enhances the moisture absorption capacity of the materials. For instance, Benmansour et al. [14] observed decreases in thermal conductivity of 87%–98% while adding 30% of date palm fibers of different sizes in a natural mortar. According to Panesar and Shindman [9], the thermal resistance of regular mortars was improved by 16% and 36% with the addition of 10% and 20% of cork, respectively. Horma et al. [12] also reported a 67% gain in the thermal resistance of a cement-based mortar while adding 10 wt% of spent tea. Charai et al. [13] reported respective decreases of 70.8% and 45.7% in the thermal conductivity and thermal diffusivity while introducing 30 wt% of spent coffee ground in a mortar. These effects are commonly linked to the low thermal conductivity of the plant fillers added, and to the rise in porosity (or the drop of density) of the resulting bio-based mortar, which alters the heat transfer characteristics.

Although the addition of plant fibers leads to improved thermophysical and even acoustic properties [2], it can negatively impact the workability of the mortar mixture and reduce the mechanical strength of the resulting bio-based composite. Due to their microporous structure and hydrophilic nature, vegetal fibers may indeed significantly impact the workability and rheology of the fresh mix by absorbing a large amount of water during mixing. Panesar & Shindman [9], Savastano et al. [15] and Chen et al. [6,16], reported that the workability of fresh mortars is significantly reduced while adding waste cork, sisal fibers or miscanthus. Besides, Hernández-Olivares et al. [17] and Li et al. [18] also noticed loss of compressive strength of mortars with the incorporation of 20 wt% of cork granules and various dosages of hemp, respectively. Similarly, Benmansour et al. [14] reported losses of compressive strength between 85% and 92% while adding 5 wt % of date palm fibers of various size in a regular concrete. This drop of mechanical properties is generally correlated with an alteration of the microstructure, as the incorporation of vegetal fibers increases the rate of macro/micro-porosities within the bio-based composite. The poor affinity between

vegetal fillers and mineral binders may also result in weak interfacial bond properties, hence contributing to this loss of mechanical strength. Besides, plant-based fibers contain extractive compounds which can be released in the fresh mortar admixture during the mixing process. In particular, sugar molecules released from the plant in the presence of water and cement may strongly impact the setting/hardening process of the cementitious matrix [19]. Indeed, several authors have shown that a small concentration of sugars is sufficient to hinder the development of cement hydration products like hydrated calcium silicate (C-S-H) and portlandite. Consequently, the setting time is generally delayed and the mechanical properties of the hardened bio-composite are negatively affected compared to those of the control mortar [20–24].

Among the wide range of plant fibers accessible in the European market, miscanthus fibers have received significant attention in recent years. Miscanthus (*x giganteus*) is a perennial rhizomatous grass that originated from East Asia and was introduced to Europe in the 1930s. This particular plant exhibits significant potential for energy and biomass generation and can be utilized as litter bedding. Importantly, its cultivation does not conflict with human or animal feeding practices [25–27]. Miscanthus can be grown for approximately 15 years, yielding an annual efficiency of 10–20 tons. It readily adapts to various climates and soil conditions, and necessitates minimal water, fertilizer, and pesticide inputs. In France, this crop is predominantly cultivated in the northern regions of the country, with efforts underway to establish an efficient value chain from the farms to the industry.

Overall, miscanthus fibers are considered to perform better than other plant fibers like straw, hemp, etc., as they exhibit good firmness and excellent thermal insulation properties. Pude et al. [28] have shown that the average composition of miscanthus fibers “consists of 40% of cellulose, 16.2% of lignin and 1.8% of silicon”. According to the same authors, “Miscanthus *x giganteus* is highly suitable to be used as aggregate for lightweight concrete, for its Young's modulus which varies between 2 and 8 GPa in the stem” [29] and for its high parenchyma content (i.e., the highly microporous cellulosic component of the plant which provides good thermal insulation). Nevertheless, only few studies have explored the feasibility and the interest of adding miscanthus fibers to cement based building materials so far [6,16,24,25,30–33]. Chen et al. [6,16] introduced presoaked miscanthus fibers into cement mortars and showed that the resulting bio-based composites exhibited large gains in thermal resistance and acoustic absorption compared to the control mortars. However, such improvements were here again obtained at the expense of mechanical properties, as the same authors reported losses of 60%–80% in the compressive strength of mortars containing 30 wt% of fibers of different lengths, in comparison with the reference. Dias and Waldmann [25] developed a protocol for manufacturing lightweight concrete masonry blocks including miscanthus aggregates, and showed that these materials provide very interesting insulation properties while retaining mechanical strength comparable to that of other lightweight concrete mixtures.

Further investigation is crucial to evaluate the potential of building materials including miscanthus fibers and consolidate

literature data regarding the thermophysical and hygric properties of this type of materials, in relation with their mechanical performance.

The objective of this study is to investigate the feasibility of incorporating micronized miscanthus fibers into a cement mortar and evaluate their influence on the thermophysical and mechanical properties of the resulting bio-composite. The utilization of micronized fibers, instead of longer fibers, aims to achieve a finer and more uniform distribution within the mortar matrix. This is undertaken with the intention of developing 3D printable materials that incorporate plant fibers, which will be addressed in subsequent parts of our project (although not covered in this particular paper).

Within the framework of this experimental program, mortar specimens including various amounts of miscanthus fibers (ranging from 0 to 7 wt% of the total composition) are first manufactured. Microstructural characterizations are then carried out on these specimens, using techniques such as scanning electron microscopy and thermo-gravimetric analysis, to assess the impact of fiber incorporation on the porous structure and the development of cement hydrates. Finally, mechanical/thermophysical properties of the mortar specimens are evaluated, and the way they change with increasing fiber content is analyzed in correlation with earlier microstructural observations.

2. Materials and methods

2.1. Materials

The plant fibers utilized in this study were provided by Addiplast Group (Saint-Pal-de-Mons, France). This product was a finely powdered form of micronized miscanthus fibers, with diameters ranging from 200 to 500 μm . It is commercially available under the reference MDDCH0114 MISCANTHUS 200–500 μm /BFF. Currently, it is mainly used in the plastic industry to manufacture bio-based composite elements for the automotive sector.

According to the manufacturer, the conditioned powder has a moisture content of 6–8 wt% and a percentage of organic matter over 94%. An interesting feature is that the

micronization process of miscanthus fibers almost eliminates the lignin component and reduces the hemicellulose content (that are respectively 0.4 and 6% in the final product), mainly retaining the cellulose content that represents about 94% of the organic composition. This latter microporous component is suited for thermal insulation applications.

In the present study, the feasibility of introducing this miscanthus powder into a cement mortar will be explored, with the objective to improve the overall thermal and hygric characteristics of the resulting material. As mentioned earlier, the utilization of micronized powder is anticipated to facilitate the even and uniform distribution of fibers within the cementitious matrix. This, in turn, presents opportunities for the development of 3D printable mortar mixes that incorporate plant fibers (although this particular aspect is not explored in the current paper). The micronized miscanthus powder was used as-received, and the fiber surface was not subjected to any chemical treatment. Fig. 1 displays two representative images of the miscanthus fibers at varying magnifications, captured through scanning electron microscopy (SEM). These images provide visual evidence of the highly microporous structure exhibited by the fibers.

A cement mortar composition available in the literature [34,35] and designed for additive manufacturing, was chosen as the reference mortar. Here again this choice was mainly guided by the 3D printability issue, which is not addressed in this paper.

This reference mix, designated M0, is based on a water-to-cement (W/C) ratio of 0.35. A combination of two different cements was used in a proportion of 93/7 parts by weight: an Ordinary Portland Cement EXTREMAT® CEM I 52.5 N-SR3 SEG containing 99% of Clinker (designated OPC) and a rapid setting Sulfo-Aluminous Cement Alpenat R² (denoted CSA), both supplied by VICAT company (L'Isle-d'Abeau, France). We adhered to the proportions of OPC and CSA cements suggested by the authors, as these ratios were determined to guarantee a good balance between extrudability and buildability, which is essential in additive manufacturing [34,35]. A superplasticizer (denoted SP) was also introduced in the mix: VISCOCRETE TEMPO 11 from SIKA Company (Baar, Switzerland). The sand was a standard siliceous sand (granular distribution specified by EN 196–1 [36], with a maximum size of 2 mm), purchased

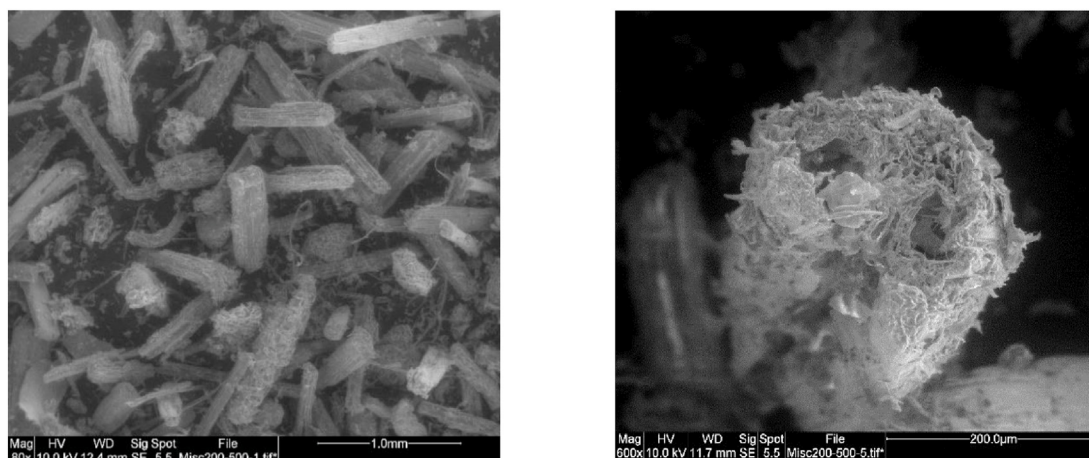


Fig. 1 – SEM pictures of the miscanthus fibers.

from S.N.L. company (Leucate, France). Table 1 provides the densities of all raw materials used in the cement mortar compositions.

This cement mortar composition is taken as model material for this study, but it is certainly not the best option in terms of sustainability due to its high clinker content. Ideally, a mineral binder with low carbon footprint should be used together with the miscanthus fibers to provide a more sustainable bio-based building material. This point should be considered in further research.

2.2. Mix design and preparation of the mortar samples

In the framework of this experimental program, different types of mortar specimens were prepared, including control specimens (M0) and mortars with various dosages of miscanthus fibers. Tables 2 and 3 displays the compositions of these mortar admixtures. For all specimens, the quantities of mineral components (OPC and CSA cements, sand) and SP remained constant, while the amounts of miscanthus fibers and water were varied. Furthermore, as we only used full bags of sand in the mixing protocol, the quantities of all component materials are given per bag of sand (of mass 1350 g) in Table 2.

Each mortar composition was labelled Mx, where x is the target dosage of as-received miscanthus fibers added to the mortar mix, expressed in wt.% of the M0 composition (i.e., the mass of miscanthus fibers divided by the total mass of all M0 components x 100). This target miscanthus content was varied in the range 0–10%. The effective mass fraction of

miscanthus fibers in the fresh mortar mix (obtained by considering the total water content in the mix, including water absorbed by fibers during a presoaking stage) is also displayed in Table 2.

Furthermore, the effective volume content of miscanthus fibers in the fresh mixes (refer to Table 2) was calculated considering an absolute density of 1570 kg/m³ for these fibers. This density value was chosen based on the findings of Chen et al. [6] and Wu et al. [37]. Indeed, Wu et al. [37] conducted experiments using helium pycnometry and determined a skeleton density of 1570 kg/m³ for a miscanthus powder extracted from the plant parenchyma, which had an average particle size of 500 µm, similar to the micronized powder utilized in this study. Additionally, Chen et al. [6] discovered that the skeleton densities of various types of miscanthus fibers (in powder form or with different particle sizes) measured by helium pycnometry were nearly identical, as all miscanthus fibers consist of cellulose, hemicellulose, and lignin, which have skeleton densities of 1559 kg/m³, 1520 kg/m³, and 1260 kg/m³, respectively. Given that the micronized miscanthus powder used in this study consists of 94% cellulose, a skeleton density close to that of cellulose is expected, and the selected value of 1570 kg/m³ can be considered as a reasonable assumption.

In order to offer the reader an inclusive collection of information, a theoretical composition of the fresh mix in kg.m⁻³ is additionally presented in Table 3.

The reason for the reported increase in water content of mortars with the amount of fibers added is due to the

Table 1 – Densities of the raw materials used in the miscanthus mortar formulations (values provided by the suppliers, except for the miscanthus fibers).

Component	Standard sand	OPC	CSA	SP	Miscanthus fibers
Density (kg m ⁻³)	2640	3190	2970	1060	1570*

* value of the skeleton density of miscanthus fibers reported by Wu et al. [37].

Table 2 – Composition of the various mortar admixtures including micronized miscanthus fibers.

Type of mortar	Sand (g)	CEM I (g)	CSA (g)	SP (g)	Miscanthus fibers* (g)	Total water** (g)	W/C ratio	Mass. fraction of miscanthus fibers (wt. %)	Vol. fraction of miscanthus fibers (vol. %)
M0	1350	1059.33	79.73	2.96	—	398.67	0.35	0	0
M2.5	1350	1059.33	79.73	2.96	72.27	604.95	0.53	2.28	3.02
M5	1350	1059.33	79.73	2.96	144.53	843.61	0.74	4.15	5.09
M7.5	1350	1059.33	79.73	2.96	216.80	1092.99	0.96	5.70	6.56
M10	1350	1059.33	79.73	2.96	289.07	1383.85	1.21	6.94	7.54

* amount of miscanthus fibers measured in the as-received state.

** the quantity of “total water” includes both the mixing water and water absorbed by miscanthus fibers at pre-soaking stage.

Table 3 – Theoretical compositions of the various miscanthus mortars in kg per m³ for the fresh mix.

Type of mortar	Sand	CEM I	CSA	SP	Miscanthus fibers	Total water
M0	1061.53	832.97	62.69	2.33	0	313.48
M2.5	885.79	695.07	52.32	1.94	47.42	396.93
M5	746.37	585.67	44.08	1.64	79.91	466.40
M7.5	641.58	503.44	37.89	1.41	103.03	519.44
M10	553.04	433.96	32.66	1.21	118.42	566.91

necessity of pre-soaking the fibers in water before mixing, as explained in the next paragraph.

In practice, the mortar samples were manufactured using an automated mortar mixer (model E092 N from Matest Spa, Treviolo, Italy). The mixing procedure adhered to the standards outlined in EN 196–1.

The mixing procedure employed for the reference mortar M0 consisted of a series of sequential steps: (1) The mixer tank was initially filled with the cement, which was a combination of OPC and CSA cements in a weight proportion of 97:3. Subsequently, the mixing water, along with the superplasticizer, was added to the tank. (2) The mixing process began at a low speed of 140 rotations per minute, and the sand was gradually introduced during the first minute. Afterward, the mortar was mixed at a high speed of 285 rotations per minute for an additional 30 s (3) Following this, the rotation was paused for 30 s to scrape the mortar from the tank's bottom. (4) A final mixing phase was then initiated at high speed, lasting for 2 min and 30 s.

Regarding the mortar formulations that include miscanthus fibers, a similar mixing protocol was employed. However, it was necessary to prepare the fibers before integrating them into the mortar mixture. Initial tests revealed that directly adding dry (as-received) fibers to the fresh mortar mix resulted in a swift absorption of the mixing water by the miscanthus fibers. These fibers possess a highly microporous structure (refer to Fig. 1) and are composed of cellulose, leading to a high absorptivity in the range of 390–500% [6]. Based on these preliminary tests and insights from a literature review, it was determined that the fibers should be soaked in water for a minimum of 2 h prior to their incorporation into the mortars (as illustrated in Fig. 2). After soaking, the fibers were placed in a fabric to eliminate excess water, and then added to the fresh mortar mix at the final stage of step (4). To ensure uniform distribution of the fibers, an additional low-speed mixing was carried out for 30 s, followed by high-speed mixing for 1 min.

Immediately after mixing, the consistency of the mortar was assessed using the Abrams mini-cone Slump test. This crucial method allows to examine the impact of adding fibers on the fresh state behavior of the mortar (consistency and flow characteristics). The slump tests were conducted according to NF EN 12350-2 standard, utilizing a mini-cone with diameters of \varnothing 5 cm at the top and \varnothing 10 cm at the base, and a

height of 15 cm. The test procedure involved filling the cone with the mortar in two layers, with each layer compacted using 12 strokes from a compacting rod. Once the top layer was compacted, we leveled the surface of the mortar by striking it off, and then the cone was carefully removed in a vertical motion. At this point, the mortar slumped (Fig. 3), and we precisely measured the distance from the top of the slumped mortar to the top of the cone.

Upon completion of the mixing procedure, the fresh mortar mixes were subsequently poured into metallic molds of varying sizes. $4 \times 4 \times 16 \text{ cm}^3$ prismatic specimens were cast for subsequent mechanical characterizations, while $4 \times 4 \times 8 \text{ cm}^3$ samples were prepared for microstructural/thermal characterizations. After a period of 24 h, the samples were removed from the molds and carefully enveloped with a plastic film. Subsequently, they were stored at a temperature of $(20 \pm 1)^\circ\text{C}$ for a duration of 28 days prior to commencing the characterizations.

2.3. Characterization methods

2.3.1. Water accessible porosity and apparent density

The evaluation of the water accessible porosity and apparent density of the hardened mortar samples followed the NF P18-459 standard [38]. Initially, $4 \times 4 \times 8 \text{ cm}^3$ specimens were sectioned into smaller samples of approximately $2 \times 2 \times 4 \text{ cm}^3$. These smaller samples were then placed in a vacuum desiccator for 4 h, followed by a 72-h immersion in water (See Fig. 4a). Upon saturation, the mass of the samples was determined in both air and water using a hydrostatic weighing setup. Subsequently, the specimens were dried in an oven at 105°C until their mass stabilized, resulting in the dry mass (See Fig. 4b). Finally, Eqs. (1) and (2) allowed to evaluate the water accessible porosity (also called apparent porosity) ε (in %) and the apparent density ρ_d (in kg/m^3), respectively:

$$\varepsilon (\%) = \frac{M_{\text{air}} - M_{\text{dry}}}{M_{\text{air}} - M_{\text{water}}} \times 100 \quad (1)$$

$$\rho_d = \frac{M_{\text{dry}}}{M_{\text{air}} - M_{\text{water}}} \times \rho_{\text{water}} \quad (2)$$

Where M_{air} and M_{water} represent the mass (in g) of the water saturated sample measured in air and in water, respectively,

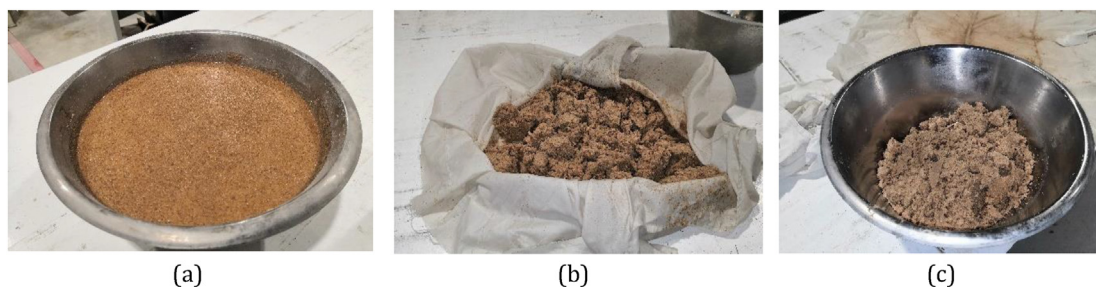


Fig. 2 – Preconditioning of miscanthus fibers: (a) soaking of fibers in water, (b) filtration with a tissue, (c) soaked fibers ready for incorporation.

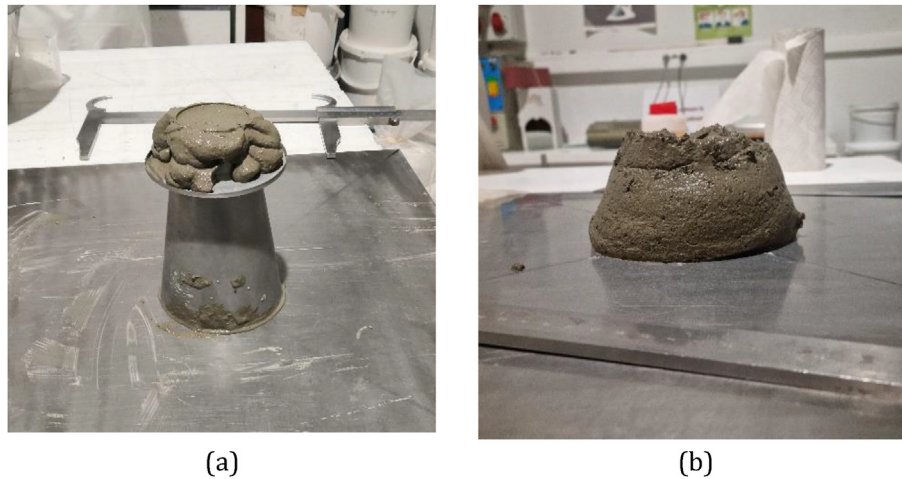


Fig. 3 – Slump test on mortars: (a) mini-cone filled with mortar, (b) slumped mortar.

M_{dry} stands for the mass of the dry sample (in g) and ρ_{water} is the density of water (in kg/m^3).

Mean values and standard deviations were calculated based on a series of three repeated tests.

2.3.2. Microstructural observations by scanning electron microscopy (SEM)

SEM characterization was carried out with a QUANTA 400 apparatus from FEI Company (Hillsboro, OR, USA), using a 20 kV electron voltage under low vacuum. Qualitative observations were performed on the micronized miscanthus powder, and on the surface of fractured mortar samples (at 28 days). To obtain the fractured surfaces, mortar specimens of dimension $4 \times 4 \times 8 \text{ cm}^3$ were broken with a hammer. The samples did not receive any metallization or chemical treatment. SEM pictures were taken both in secondary electron mode (SE) and in backscattered electron mode (BSE).

2.3.3. Thermogravimetric analysis (TGA)

Thermogravimetric analyses (TGA) were conducted on small samples of the miscanthus powder, and on fine powders of

the different mortars (obtained by grinding and sieving below $315 \mu\text{m}$). The TGA technique consists in monitoring the weight loss of the sample during a ramp of temperature, in order to detect any degradation of organic or mineral compounds, which allows to obtain quantitative information on the composition of the sample.

These experiments were made using a STA449 apparatus from NETZSCH Company (Selb, Germany). The samples were subjected to ramps of temperature from 25°C to 1250°C at a heating rate of 10°C/min and under nitrogen flow (50 ml/min). Three tests were carried out for each type of material.

2.3.4. Mechanical characterizations of hardened mortars

The hardened bio-based mortars were tested at 28 days, in accordance with EN 196-1 standard [36]. A press of capacity 300 kN was used for these characterizations (model Pilot Pro from Controls S. p.a., Italia).

$4 \times 4 \times 16 \text{ cm}^3$ specimens (series of 6 for each type of mortar) were first tested under 3-point bending configuration to evaluate the flexural strength (Fig. 5 a.). After breakage, the twelve half samples were retrieved and tested in compression (Fig. 5b and 5c).

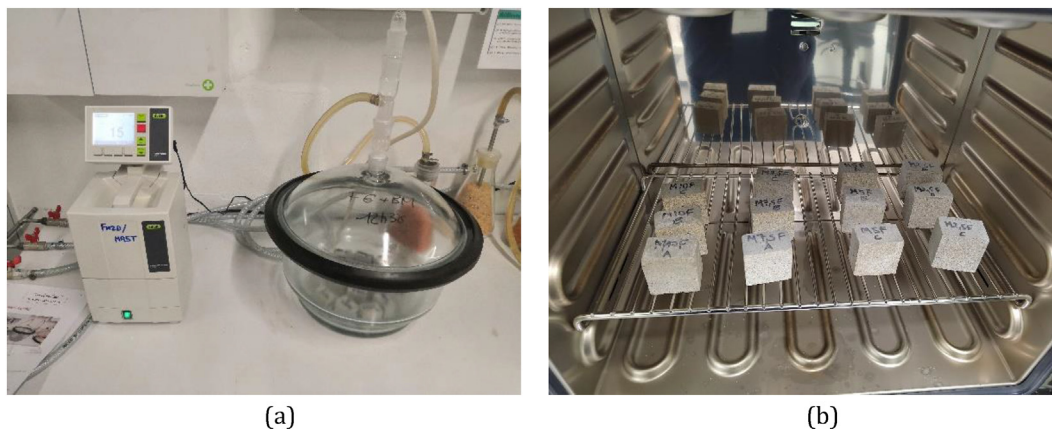


Fig. 4 – Determination of the water accessible porosity and apparent density of mortar: (a) Vacuum packing of samples and imbibition with water, (b) Conditioning at 105°C .

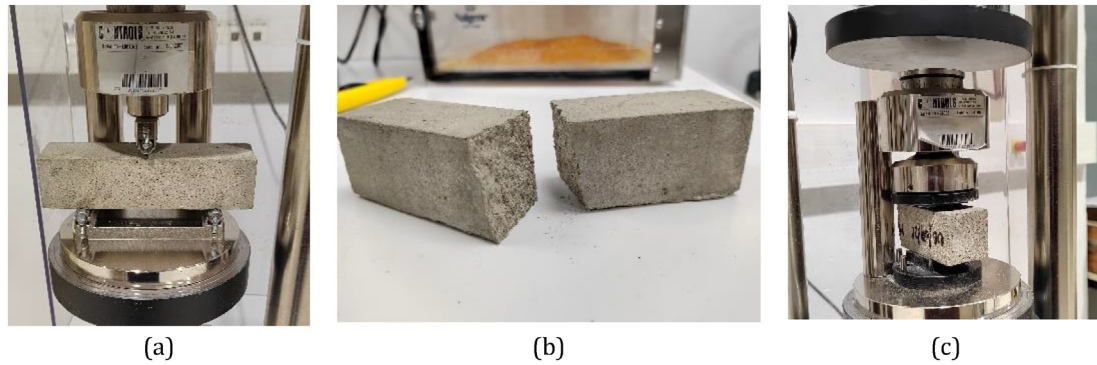


Fig. 5 – Mechanical characterization of the mortar samples: (a) 3-point bending configuration, (b) broken specimen (c) half sample tested in compression.

2.3.5. Characterization of thermophysical properties

The Hot Disk method, denoted HD, made it possible to quantify several thermophysical properties of the bio-based mortars. A TPS 2500 S apparatus from Hot Disk Company (Gothenburg, Sweden) was used for these experiments. The device comprises a Kapton insulated probe (with a radius of 6.4 mm) connected to a thermal constant analyzer.

The HD technique is based on the theory of transient plane source as per ISO 22007–2 [39] standard. A double spiral shaped sensor element is inserted between two samples of the material to be tested (mortar prisms in the present case) that are considered infinite in all directions with respect to the size of the sensor. This sensor not only functions as a heat source to raise the temperature of the sample, but also as a resistance thermometer to record the temperature increase over time. The HD device illustrated in Fig. 6 allows for quick, precise, and non-destructive assessment of three key thermal properties of a sample: thermal conductivity (represented by λ ,

measured in $\text{W}\cdot\text{m}^{-1}\cdot\text{K}^{-1}$), thermal diffusivity (α in $\text{m}^2\cdot\text{s}^{-1}$), and volumetric heat capacity ($\rho\cdot\text{Cp}$ in $\text{J}\cdot\text{m}^{-3}\cdot\text{K}^{-1}$).

To ensure accurate measurement of thermophysical properties of porous building materials, it is crucial to control the impact of variables such as temperature and moisture content. Therefore, the samples underwent a week-long conditioning period at 20 °C and 50% relative humidity (RH) to reach a stable state before testing. During the characterization, the entire experimental setup (sensor placed between the 2 prismatic specimens) was kept in a climate-controlled chamber to maintain consistent temperature and humidity levels (see Fig. 6). In practice, HD measurement was carried at several fixed temperatures over the range 10–45 °C, while a constant humidity level of 50% RH was set in the chamber.

Finally, one should keep in mind that for a specific configuration (material type, temperature and relative humidity), the manufacturer of the HD instrument advises obtaining the thermal properties (λ , α , and $\rho\cdot\text{Cp}$) of the sample

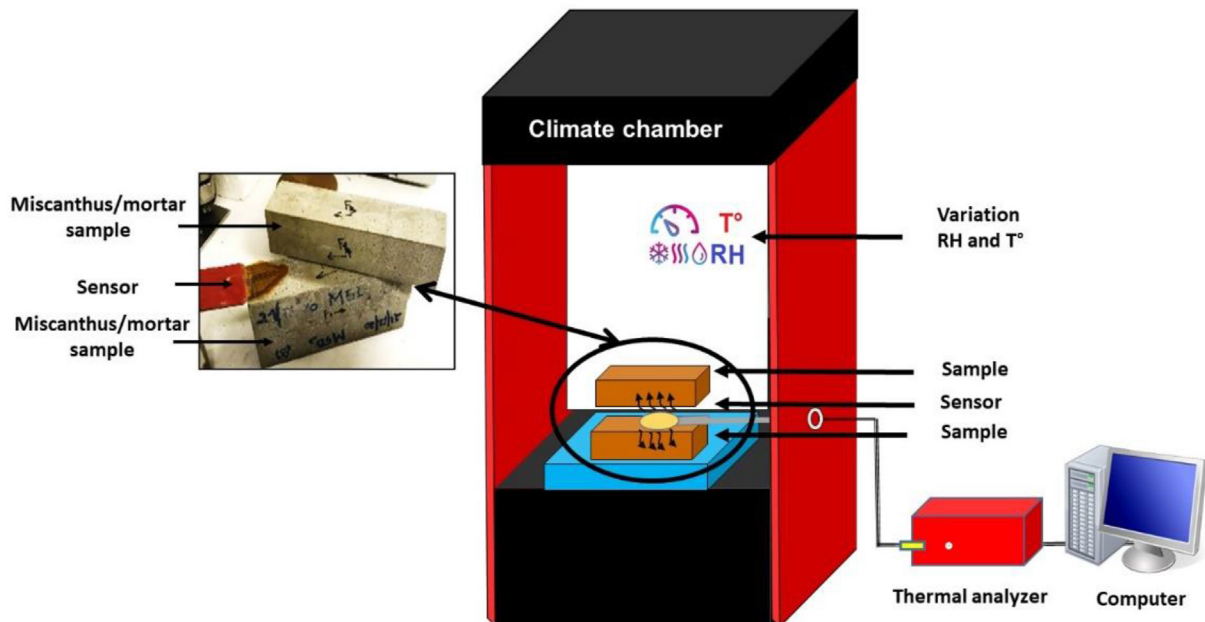


Fig. 6 – Experimental setup used to measure thermophysical properties of mortars.

in one single measurement. They guarantee an accuracy of better than 5% and reproducibility of better than 1%, based on multiple tests on standard materials [40]. In the present work, values were averaged on three repeated measurements, and uncertainties were derived from standard deviations. In general, these uncertainties were below the 5% level stated by the manufacturer.

3. Results and discussion

3.1. Influence of miscanthus fibers on the workability of the fresh mortar mixes

In order to assess the impact of miscanthus fibers on the workability of fresh mortars, slump tests were conducted using the Abrams mini-cone method. Fig. 7 illustrates the relationship between slump values and the concentration of miscanthus fibers in the mortar mixes. A linear fit yields a R^2 coefficient exceeding 0.99, clearly illustrating the direct correlation between the slump and the fiber content.

Despite the pre-saturation of miscanthus fibers with water prior to their inclusion in the mortar mix (as described in the pre-soaking sequence in section 2.2.), a noticeable reduction in mortar workability can be observed with increasing fiber content. This decrease in workability cannot be solely attributed to the absorptive nature of the fibers since they were pre-soaked to prevent water absorption during mixing. Instead, it is likely a consequence of alterations in the granular distribution within the mortar mix [6,9,15,16,41,42].

Similar patterns have been observed by various researchers in the context of different bio-based mortars. Chen et al. [6,16] observed a decrease in workability when miscanthus fibers were incorporated into ultra-lightweight concrete. Mansur and Aziz [42] noted that the addition of jute fibers influenced the workability of mortars. Additionally, Savastano et al. and Panesar & Shindman reported similar trends in mortars containing sisal fibers and waste cork, respectively [9,15].

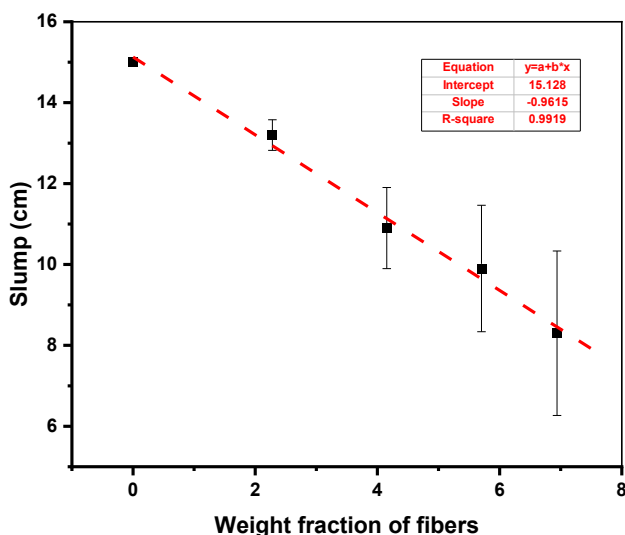


Fig. 7 – Slump of the bio-based mortar mixes as function of their miscanthus fiber content.

3.2. Microstructural characterizations

3.2.1. SEM observations

Fig. 8 displays the microstructure of the various hardened mortars, as observed by Scanning Electron Microscopy in backscattered electron mode (BSE). Images at two different magnifications ($\times 80$ and $\times 300$) are provided.

Concerning the reference mortar M0, the pictures (Fig. 8a and 8a') show smooth surfaces that are characteristic of a dense microstructure with moderate porosity. The use of BSE

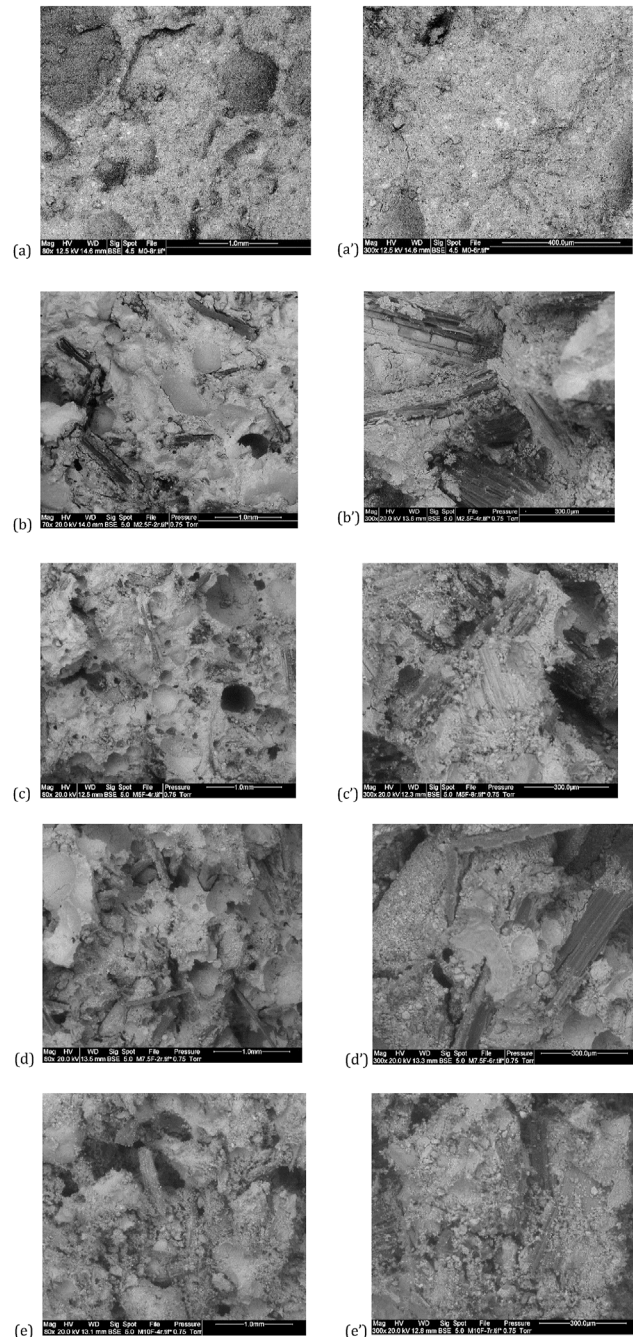


Fig. 8 – Microstructural examination of the different mortars using SEM images in BSE mode and at varying magnifications: (a)-(a') M0, (b)-(b') M2.5, (c)-(c') M5, (d)-(d') M7.5, and (e)-(e') M10.

imaging provides chemical contrast which enables the detection of few small and white inclusions, indicating anhydrous cement grains. This is an indication that hydration reactions are still ongoing even after 28 days of curing.

The introduction of miscanthus fibers into the mortar results in an increased porosity of the hardened materials, consistent with findings reported in other studies in the literature [16,22]. Many cavities can be observed, possibly resulting from the evaporation of water absorbed by the fibers at the presoaking stage or related to the air trapped during mixing.

Furthermore, the pictures reveal that fractured surfaces display progressively a more flaky/powdery aspect, with the presence of many debris and dust. This feature suggests that the material becomes less cohesive and more friable as the fiber content is increased.

Regarding the fiber distribution within the mortars, images at low magnification show that there is a rather uniform fiber arrangement. Besides, on some pictures (for instance Fig. 8 b' and d'), the surface of the miscanthus fibers appears very clean and smooth which suggests limited interactions between the vegetal fibers and the mineral matrix. The reason for this could be the lack of prior treatment applied to the surface of the fibers before utilization. Some authors have shown that complementary chemical treatments (alkali or silane) [19] or thermal treatments [24] of the plant fibers can improve the bond properties with the mineral matrix.

3.2.2. Thermogravimetric analyses (TGA)

TGA analyses were carried out following the protocol detailed in section 2.3.3. Figs. 9 and 10 display respectively, the typical mass loss curves during a 10 °C/min temperature ramp and the first derivative signals (DTG) for the different mortars. Several degradations phases can be observed on these curves, which are closely related to the mortar compositions.

In reference to the M0 mortar, three recognizable stages are observed, indicative of the products generated through hydration reactions between the OPC/CSA cements and water [43–45].

- The first sign of weight loss is noticeable between 30 and 130 °C and is also indicated by peak A on the DTG signal. It results from both the evaporation of capillary water and the elimination of water associated with ettringite hydrate,
- The reduction in weight occurring between 130 and 400 °C can be attributed to the release of water present in hydrated calcium silicates (C-S-H). The B shoulder on the DTG signal in the 160–240 °C range specifically indicates the dehydration of calcium mono-carboaluminate (AFm),
- The decrease in mass observed between 400 and 540 °C, also indicated by peak C in the DTG curve, relates to the dehydroxylation of portlandite ($\text{Ca}(\text{OH})_2$),
- Finally, the mass loss in the temperature interval of 600–800 °C (and peak D in the DTG signal) corresponds to the decarbonation of calcium carbonate. Given that this temperature range is relatively lower than the typical decomposition range for stable carbonate forms, which generally occurs between 750 and 900 °C, it is likely related to poorly crystallized carbonate compounds [46,47].

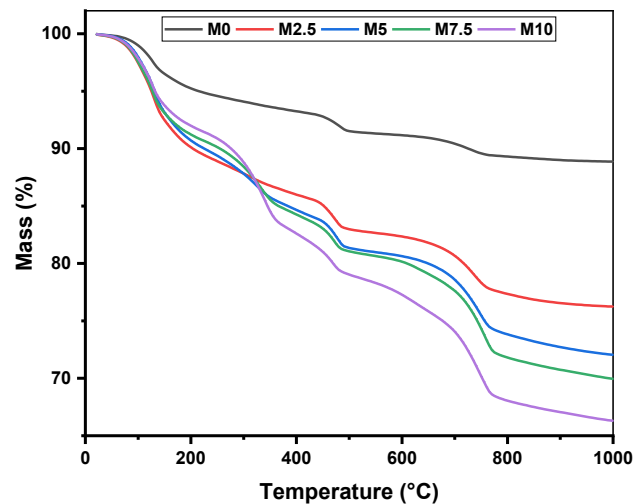


Fig. 9 – Typical TGA curves (mass loss) recorded at 10 °C/min for the different mortars.

In regard mortar formulations including miscanthus fibers, specific features can be pointed out:

- TGA results indicate that the overall weight loss at 900 °C is significantly higher in comparison to mortar M0 and that this difference becomes more pronounced as the fiber content increases. This can be attributed to the evaporation of surplus water used to pre-soak the fibers and preserve the workability of the mortars, as well as the degradation of the miscanthus fibers overheating,
- The degradation trends of the bio-based mortars, as depicted in their DTG curves, are similar to those previously seen for mortar M0. This indicates the presence of the same cement hydrates, such as ettringite, AFm, portlandite, and calcium carbonate hydrates. A noteworthy difference is the heightened amplitude of peak D, indicating a higher relative proportion of calcium carbonate.

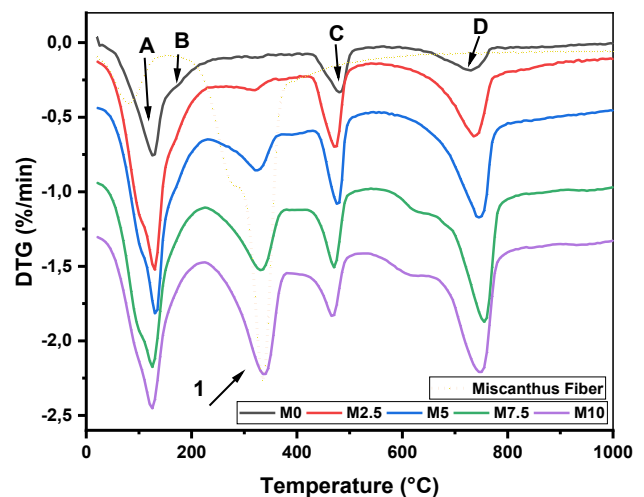


Fig. 10 – Typical DTG curves (first derivative signals) of the different mortars at 28 days. The curve recorded for neat miscanthus fibers is also superimposed for comparison (in dotted line).

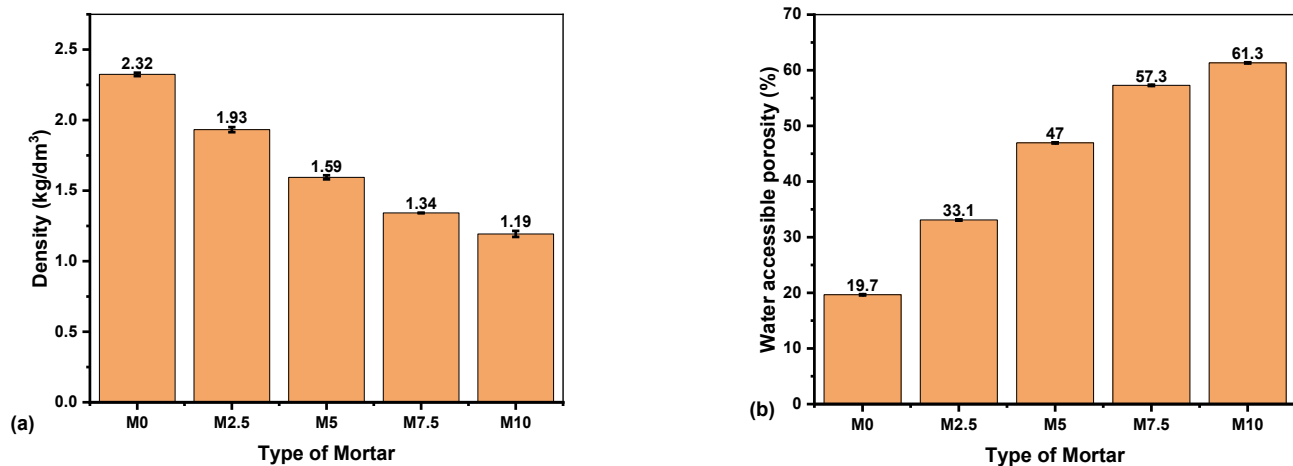


Fig. 11 – Mean values of (a) the apparent density and (b) the water accessible porosity for the different mortars studied at 28 days.

This can be attributed to the greater porosity, as demonstrated through SEM analysis, which makes these bio-based mortars more susceptible to carbonation. The amplitude of DTG peak A in the bio-based mortars is also significantly higher compared to reference M0, likely due to the evaporation of residual water from the miscanthus fibers (this water was absorbed by the fibers at presoaking stage). Besides, the amplitude of DTG peak C related to portlandite was not reduced after incorporating the miscanthus fibers, even appearing higher in M2.5 and M5 mortars compared to the reference material. This result suggests that there was no negative impact of sugar molecules extracted from the fibers on the cement hydration, possibly due to filtering the presoaked fibers to remove excess water before adding them to the mortar mixture (this would have removed the extracted sugar molecules). Additionally, the micronized miscanthus fibers contain a low hemicellulose content compared to larger fibers. Since sugars are primarily derived from hemicellulose compounds [19], this may account for the lack of noticeable effects.

- Besides, DTG curves show a new peak (peak 1 around 350 °C in Fig. 10) that was not present in the reference mortar. This peak becomes more prominent with the addition of fibers and appears to be a result of the thermal decomposition of miscanthus fibers (as indicated by comparison with the DTG signal of the neat fibers, shown as a dotted line). It is very likely that the surface area of peak is proportional to content of miscanthus fibers. The peak position is also consistent with the decomposition temperature range of cellulose (between 325 and 400 °C) [24] which is the main component of micronized miscanthus fibers. Lignin decomposes at higher temperature between 300 and 550 °C [48], but its content is very limited in the micronized powder.

3.2.3. Dry density and water accessible porosity

Diagrams displayed in Fig. 11a and b show respectively the mean values (and corresponding standard deviations) of the

apparent density and water accessible porosity of the bio-based mortars at 28 days (see protocol in section 2.3.1, based on NF P18-459 standard). Fig. 12 represents the evolutions of the same quantities as a function of the mass fraction of miscanthus fibers in the mortars.

The inclusion of miscanthus fibers in mortars leads to a nearly linear decrease in apparent density. Conversely, the water-accessible porosity increases with the content of miscanthus fibers. This supports the finding of increased porosity seen in SEM images (refer to section 3.2.1).

Multiple authors have reported comparable tendencies regarding the effects of several plant fibers on the density and porosity of bio-based mortars [6,16,22,24,25]. These effects are generally assigned to various mechanisms:

- The low density of miscanthus fibers compared to the mineral components (cement, sand) results in a decrease in density of the bio-based mortars,

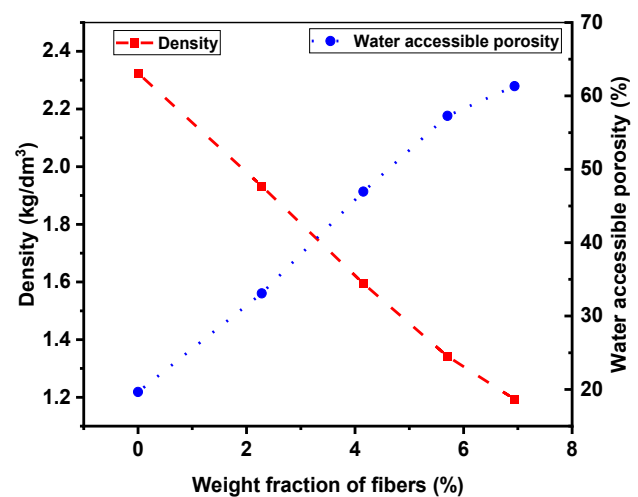


Fig. 12 – Dependence of the apparent density/the water accessible porosity of mortars (at 28 days) on the miscanthus fiber content.

- The incorporation of fibers also modifies the granular distribution and internal packing of mortars,
- The porosity within fibers and at the interface between fibers and cementitious matrix also raises the overall porosity of mortars, contributing to the decrease in density. The pre-saturation of fibers in water may also contribute to the overall porosity of the mortar, especially when this excess water evaporates.

3.3. Mechanical properties

Fig. 13 presents the mean values of flexural and compressive strengths at 28 days for the bio-based composites, obtained respectively from 6 to 12 repeated tests (as outlined in section 2.3.4). The diagrams also include error bars that indicate the standard deviations. The relationship between the weight content of miscanthus fibers in the specimens and the strength values is visualized in Fig. 14.

Overall, both flexural and compressive strengths of the bio-based composites exhibit a substantial decrease upon the incorporation of miscanthus fibers (Fig. 14). Furthermore, among these two properties, the compressive strength seems to be the most affected, as the addition of 2.28 wt % of miscanthus fibers in the mortar (corresponding mortar M2.5) results in a 70% strength loss (from 72 MPa to 21 MPa). Similarly, the compressive strength values of mortars containing fiber contents exceeding 4.15 wt% (M5, M7.5, and M10) fall below the minimum specification for structural concrete (17.2 MPa) [49], which makes them unsuitable for structural applications.

A similar drop of mechanical strength of bio-based mortars was reported by multiple authors with the addition of various type of vegetal fibers. As an example, Chen et al. [6] found that the compressive strength of cement composites incorporating 30 wt% miscanthus fibers of various lengths (which were pre-soaked in water) decreased by 60–80% compared to pure cement paste. Research conducted by Benmansour et al. revealed a decrease of 85–92% in the compressive strength of

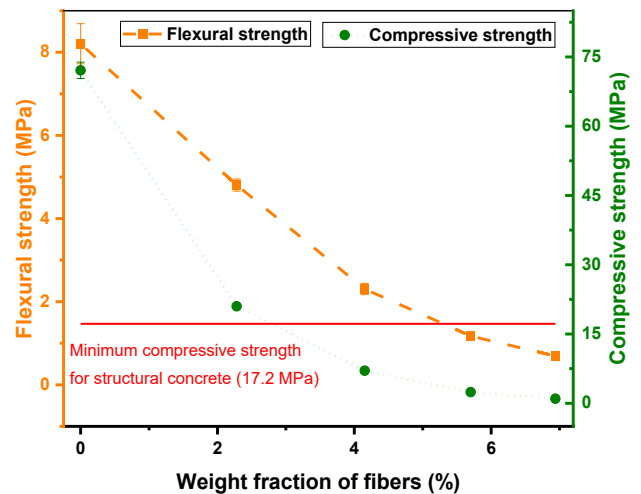


Fig. 14 – Flexural and compressive strengths versus weight fraction of miscanthus fibers in the mortars.

concrete upon the addition of 5 wt% date palm fibers [14]. Similar trends were observed by Hernández-Olivares et al. [17] and Li et al. [18], who noted a decline in compressive strength when incorporating 20 wt% cork granules in a gypsum composite and hemp fibers in concrete, respectively.

The decline in the mechanical performance of bio-based mortars observed in this study can be attributed to several factors, in line with the findings of other authors [6,7,16–18,22,25]. These factors include: i) a significant reduction in the bulk density of the mortar due to the introduction of numerous pores, voids, and entrapped air with the incorporation of vegetal fibers; ii) the fibers can behave like voids when subjected to mechanical loads due to their lightweight nature; iii) bond defects between the fibers and the cement matrix can act as weak points, thereby contributing to the initiation and propagation of cracks and leading to an overall loss of strength in the bio-based composites.

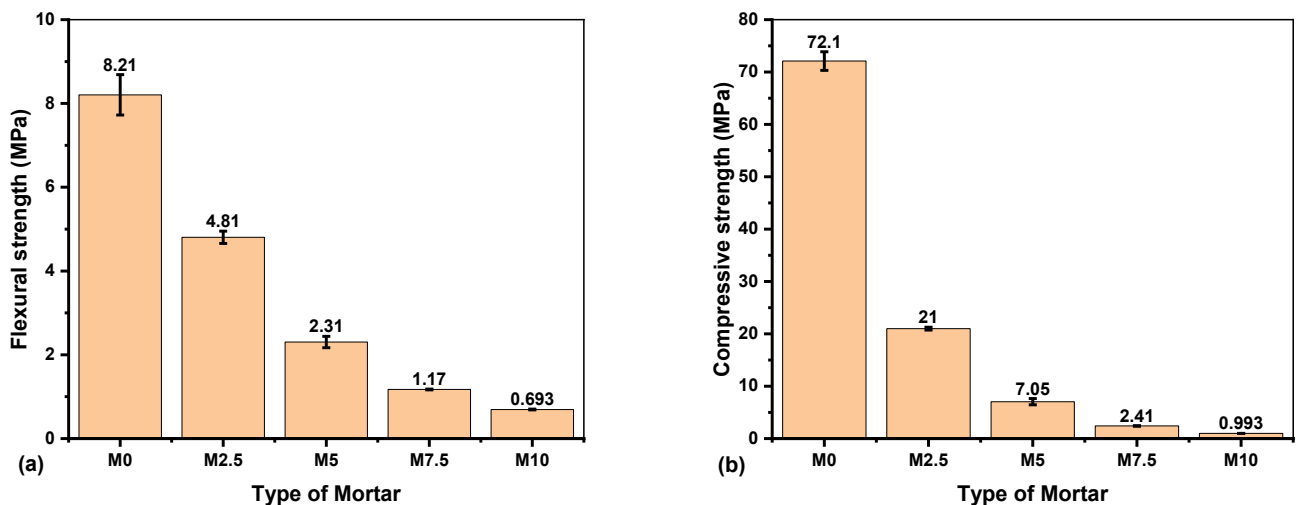


Fig. 13 – Mechanical properties of the different mortars at 28 days: (a) Flexural and (b) compressive strengths.

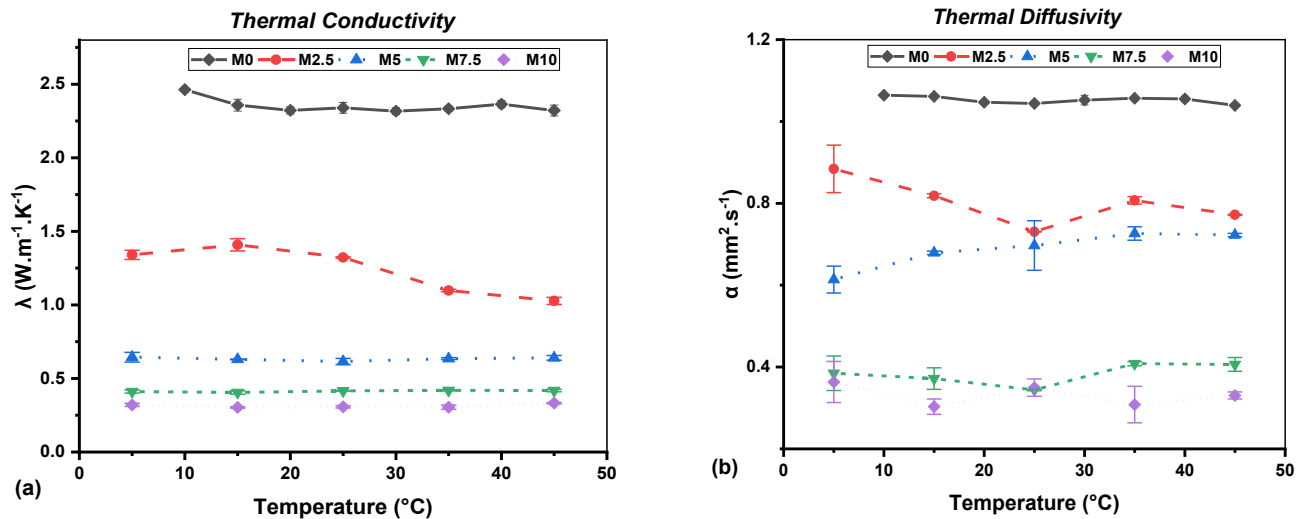


Fig. 15 – Temperature dependence of (a) thermal conductivity and (b) thermal diffusivity for the different bio-based mortars.

3.4. Thermophysical properties

Fig. 15a and b depict respectively the changes in thermal conductivity (λ) and thermal diffusivity (α) upon temperature for the different bio-based mortars, with error bars indicating standard deviations. The Hot-disk method, detailed in section 2.3.5., was employed to perform the measurements under controlled humidity condition (50% RH) and across a broad range of temperatures (5–45 °C). The results are an average of three repeated measurements.

For reference mortar M0, the thermal conductivity (λ) and thermal diffusivity (α) values measured at 25 °C are $2.34 \text{ W m}^{-1} \text{ K}^{-1}$ and $1.04 \text{ mm}^2 \text{ s}^{-1}$, respectively, and are in line

with those reported by Shafigh et al. for similar-density OPC mortars [50]. Additionally, thermal properties exhibit minimal variation from 10 °C to 45 °C, as per the experimental uncertainties, in agreement with previous literature [51].

Besides, as seen in Fig. 15, the incorporation of miscanthus fibers results in a noticeable reduction in both thermal conductivity and thermal diffusivity. Overall, the greater the fiber content, the lower the thermal conductivity of the mortar composites (as indicated by the downward shift of the curves).

Furthermore, Fig. 16 illustrates the impact of miscanthus fiber content on the thermal conductivity at 25 °C of the bio-based composites.

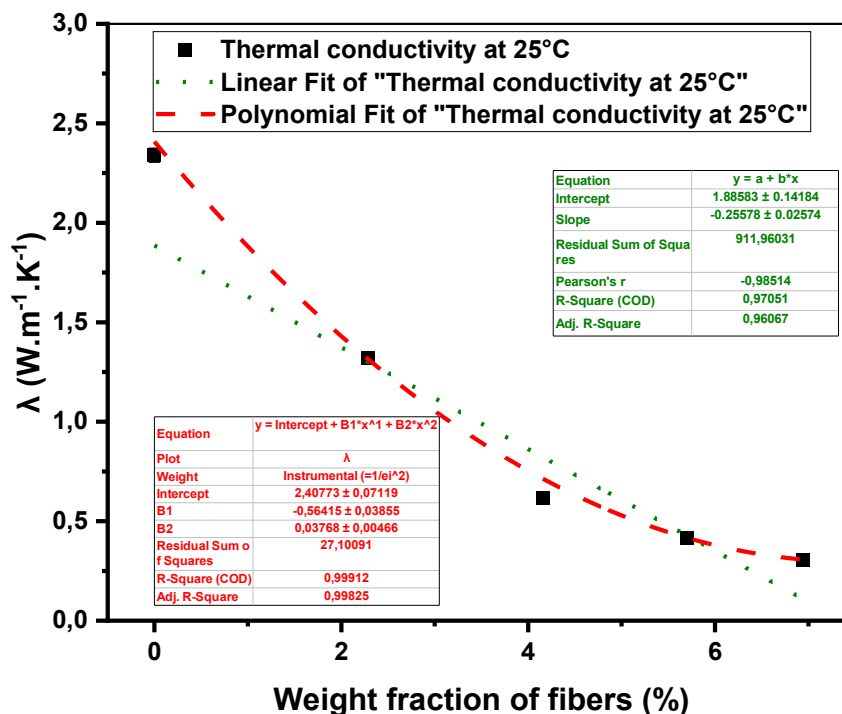


Fig. 16 – Thermal conductivity of mortars (at 25 °C) versus weight content of miscanthus fibers.

The results demonstrate a nearly linear decrease in thermal conductivity with increasing fiber content, as evidenced by a high R^2 coefficient (above 0.97) for the regression line. This trend has been observed by various researchers for different types of mortars containing vegetal fibers [5,7,9,10]. The same authors have also reported that an even stronger correlation can be achieved through a polynomial fit, and this holds true in our current context, as depicted in Fig. 16.

Incorporating just 5.7 wt% of fibers in the mortars caused a nearly 82% reduction in thermal conductivity, making the material highly suitable for insulation purposes. Benmansour et al. [14] observed a similar trend, with a decrease of 87–98% in thermal conductivity when adding 30% of different sized date palm fibers to natural cement mortar. Similarly, Panesar & Shindman [9] found a substantial drop in the thermal conductivity of concrete when incorporating waste cork.

Additionally, Fig. 17 illustrates the correlation between the thermal conductivity at 25 °C and the density of the bio-based mortars. Here again, a quasi-linear trend is observed with a R^2 coefficient of the regression line higher than 0.98, but a polynomial fit is also effective with a R^2 coefficient higher than 0.99. This finding is in agreement with the literature [2,7,16,52–54], as numerous authors have established a direct correlation between these two quantities for mortars including different types of vegetal fibers.

In conclusion, the reduction in conductivity of bio-based mortars can be attributed to the low conductivity of the incorporated plant fibers (Schnabel et al. [55] reported a value $0.04 \text{ W m}^{-1} \text{ K}^{-1}$ in the case of miscanthus) and to the increased overall porosity. It is also suggested that heat transfer through conduction is supplanted by natural convection in the porous phase [2,7,9,18,41,56].

Finally, Fig. 18 depicts the variation with temperature of the volumetric specific heat capacity ($\rho \cdot C_p$) for the different mortars. Here again only little variation of this property is observed over the temperature range studied, but a substantial reduction of the $\rho \cdot C_p$ level is obtained with the addition of miscanthus fibers (the curves are globally shifted downward when the fiber content increases). The main reason behind this effect is probably the large reduction in density of the bio-based mortars as the fiber content is increased.

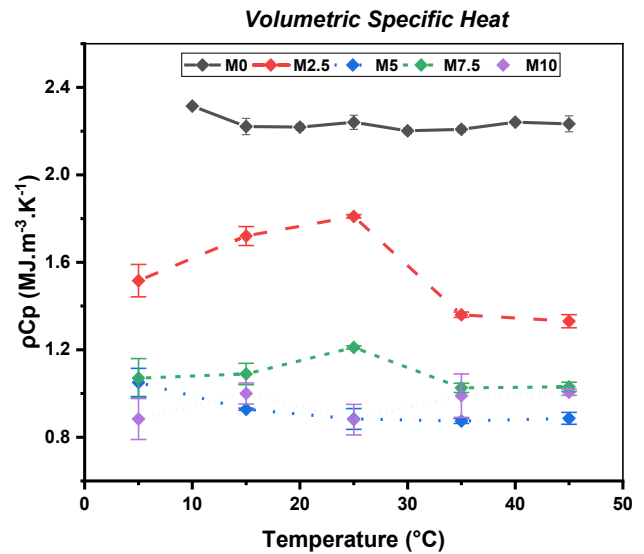


Fig. 18 – Temperature dependence of the volumetric heat capacity for the different mortars.

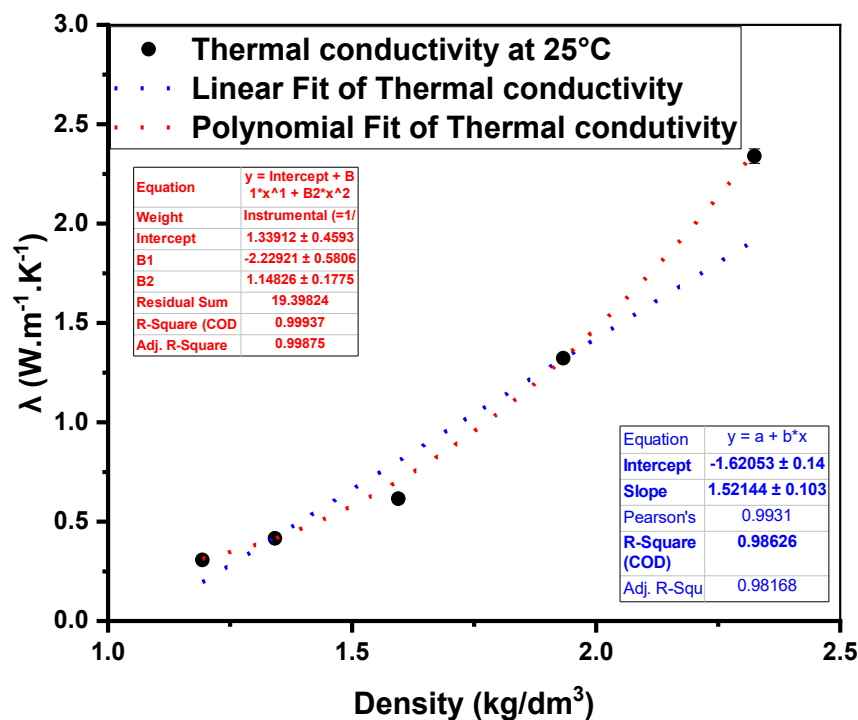


Fig. 17 – Thermal conductivity (at 25 °C) versus density of mortars.

4. Conclusion

This study aimed to investigate the potential of incorporating micronized miscanthus fibers into cement mortar formulations and assess its impact on the microstructure, mechanical properties, and thermophysical characteristics of the resulting bio-based composites.

The initial finding revealed a noticeable decrease in the workability of mortars upon fiber addition, despite the pre-saturation of fibers with water. This effect was primarily attributed to the modification of the overall granular distribution and packing density within the mortar mixes. Therefore, the pre-soaking of miscanthus fibers in water was deemed necessary during the manufacturing process of the bio-based mortar specimens.

Microstructural characterizations were then carried out at 28 days on the different mortars. SEM observations revealed that micronized fibers are rather homogeneously distributed within the mortar matrix but suggested a reduction of the material cohesiveness upon fiber addition. An almost linear increase in the overall material porosity, resulting in a reduction of density, was observed as the fiber content was increased. This effect was mainly assigned to the air trapped during mixing and to microporosities formed after evaporation of the excess water absorbed by the vegetal fibers at presoaking stage.

The porosity was deemed to be the primary factor that led to a decline in the mechanical strength of bio-based composites under both flexural and compression tests. However, even the addition of small amounts of plant fibers led to a significant improvement in the material's thermal resistance.

Ultimately, this study yields noteworthy insights into the potential utilization of the bio-based mortars:

- Mortar M2.5, containing 2.28 wt % of fibers, meets the criteria for structural applications as it maintains a compressive strength above the minimum requirement. However, the improvement in thermal resistance is relatively modest, reaching only about 40%
- Mortars containing dosages of fibers exceeding 4.15 wt% exhibit significant enhancement in thermal resistance, surpassing 70% compared to the plain mortar. These mortars maintain satisfactory mechanical properties for handling and are well-suited for insulation applications.

The hygric properties of these bio-based composites will also be investigated in a next research. This is an important issue, since the comfort of building users does not only depend on thermal conditions but also on the ability of building materials to regulate moisture of the indoor environment. Furthermore, additional investigations are needed at the wall scale, to obtain data that more accurately reflect actual building usage scenarios.

Funding

The funding for this research was provided by Labex MMCD (Multi-Scale Modelling & Experimentation of Materials for

Sustainable Construction), as part of the ANR Investments for the Future program (ANR-11-LABX-022-01).

Declaration of competing interest

The authors declare that they have no known competing financial interests or personal relationships that could have appeared to influence the work reported in this paper.

Acknowledgements

The authors would like to acknowledge Vicat Company for providing the OPC and Alpenat cements, and Addiplast Group for supplying the micronized miscanthus fibers. In addition, they would like to thank Dr Myriam Duc for her assistance regarding SEM experiments.

REFERENCES

- [1] International Energy Agency (IEA), Tracking buildings 2021, Paris, 2021. <https://www.iea.org/reports/tracking-buildings-2021>.
- [2] Amziane S, Sonebi M. Overview on biobased building material made with plant aggregate. RILEM Technical Letters 2016;1:31–8. <https://doi.org/10.21809/rilemtechlett.2016.9>.
- [3] Chel A, Kaushik G. Renewable energy technologies for sustainable development of energy efficient building. Alex Eng J 2018;57:655–69. <https://doi.org/10.1016/j.aej.2017.02.027>.
- [4] Amziane S, Collet F, editors. Bio-aggregates based building materials: state-of-the-art report of the RILEM technical committee 236-BBM. Dordrecht: Springer Netherlands; 2017. <https://doi.org/10.1007/978-94-024-1031-0>.
- [5] Ashour T, Wieland H, Georg H, Bockisch F-J, Wu W. The influence of natural reinforcement fibres on insulation values of earth plaster for straw bale buildings. Mater Des 2010;31:4676–85. <https://doi.org/10.1016/j.matdes.2010.05.026>.
- [6] Chen Y, Yu QL, Brouwers HJH. Acoustic performance and microstructural analysis of bio-based lightweight concrete containing miscanthus. Construct Build Mater 2017;157:839–51. <https://doi.org/10.1016/j.conbuildmat.2017.09.161>.
- [7] Chikhi M, Agoudjil B, Boudenne A, Gherabli A. Experimental investigation of new biocomposite with low cost for thermal insulation. Energy Build 2013;66:267–73. <https://doi.org/10.1016/j.enbuild.2013.07.019>.
- [8] Liu X, Chia KS, Zhang M-H. Development of lightweight concrete with high resistance to water and chloride-ion penetration. Cement Concr Compos 2010;32:757–66. <https://doi.org/10.1016/j.cemconcomp.2010.08.005>.
- [9] Panesar DK, Shindman B. The mechanical, transport and thermal properties of mortar and concrete containing waste cork. Cement Concr Compos 2012;34:982–92. <https://doi.org/10.1016/j.cemconcomp.2012.06.003>.
- [10] Haba B, Agoudjil B, Boudenne A, Benzarti K. Hygric properties and thermal conductivity of a new insulation material for building based on date palm concrete. Construct Build Mater 2017;154:963–71. <https://doi.org/10.1016/j.conbuildmat.2017.08.025>.

- [11] Chennouf N, Agoudjil B, Boudenne A, Benzarti K, Bouras F. Hygrothermal characterization of a new bio-based construction material: concrete reinforced with date palm fibers. *Construct Build Mater* 2018;192:348–56. <https://doi.org/10.1016/j.conbuildmat.2018.10.089>.
- [12] Horma O, Charai M, El Hassani S, El Hammouti A, Mezrhab A. Thermo-physical and mechanical characterization of cement-based mortar incorporating spent tea. *J Build Eng* 2022;52:104392. <https://doi.org/10.1016/j.job.2022.104392>.
- [13] Charai M. Thermophysical characteristics of cement-based mortar incorporating spent coffee grounds. *Mater Today* 2022;4.
- [14] Benmansour N, Agoudjil B, Gherabli A, Kareche A, Boudenne A. Thermal and mechanical performance of natural mortar reinforced with date palm fibers for use as insulating materials in building. *Energy Build* 2014;81:98–104. <https://doi.org/10.1016/j.enbuild.2014.05.032>.
- [15] Savastano H, Agopyan V, Nolasco AM, Pimentel L. Plant fibre reinforced cement components for roofing. *Construct Build Mater* 1999;13:433–8. [https://doi.org/10.1016/S0950-0618\(99\)00046-X](https://doi.org/10.1016/S0950-0618(99)00046-X).
- [16] Chen YX, Wu F, Yu Q, Brouwers HJH. Bio-based ultra-lightweight concrete applying miscanthus fibers: acoustic absorption and thermal insulation. *Cement Concr Compos* 2020;114:103829. <https://doi.org/10.1016/j.cemconcomp.2020.103829>.
- [17] Hernández-Olivares F, Bollati MR, del Rio M, Parga-Landa B. Development of cork–gypsum composites for building applications. *Construct Build Mater* 1999;13:179–86. [https://doi.org/10.1016/S0950-0618\(99\)00021-5](https://doi.org/10.1016/S0950-0618(99)00021-5).
- [18] Li Z, Wang X, Wang L. Properties of hemp fibre reinforced concrete composites. *Compos Appl Sci Manuf* 2006;37:497–505. <https://doi.org/10.1016/j.compositesa.2005.01.032>.
- [19] Boix E, Gineau E, Narciso JO, Höfte H, Mouille G, Navard P. Influence of chemical treatments of miscanthus stem fragments on polysaccharide release in the presence of cement and on the mechanical properties of bio-based concrete materials. *Cement Concr Compos* 2020;105:103429. <https://doi.org/10.1016/j.cemconcomp.2019.103429>.
- [20] Wei J, Ma S, Thomas DG. Correlation between hydration of cement and durability of natural fiber-reinforced cement composites. *Corrosion Sci* 2016;106:1–15. <https://doi.org/10.1016/j.corsci.2016.01.020>.
- [21] Doudart de la Grée GCH, Yu QL, Brouwers HJH. Assessing the effect of CaSO₄ content on the hydration kinetics, microstructure and mechanical properties of cements containing sugars. *Construct Build Mater* 2017;143:48–60. <https://doi.org/10.1016/j.conbuildmat.2017.03.067>.
- [22] Le Ngoc Huyen T, Queneudec T Kint M, Remond C, Chabbert B, Dheilly R-M. Saccharification of *Miscanthus x giganteus*, incorporation of lignocellulosic by-product in cementitious matrix. *Comptes Rendus Biol* 2011;334:837.e1–837.e11. <https://doi.org/10.1016/j.crv.2011.07.008>.
- [23] Kochova K, Schollbach K, Gauvin F, Brouwers HJH. Effect of saccharides on the hydration of ordinary Portland cement. *Construct Build Mater* 2017;150:268–75. <https://doi.org/10.1016/j.conbuildmat.2017.05.149>.
- [24] Wu F, Yu Q, Brouwers HJH. Long-term performance of bio-based miscanthus mortar. *Construct Build Mater* 2022;324:126703. <https://doi.org/10.1016/j.conbuildmat.2022.126703>.
- [25] Dias PP, Waldmann D. Optimisation of the mechanical properties of *Miscanthus* lightweight concrete. *Construct Build Mater* 2020;258:119643. <https://doi.org/10.1016/j.conbuildmat.2020.119643>.
- [26] Lewandowski I, Clifton-Brown J, Kiesel A, Hastings A, Iqbal Y. 2- *miscanthus*. In: Alexopoulou E, editor. *Perennial grasses for bioenergy and bioproducts*. Academic Press; 2018. p. 35–59. <https://doi.org/10.1016/B978-0-12-812900-5.00002-3>.
- [27] Lewandowski I, Heinz A. Delayed harvest of *miscanthus*—influences on biomass quantity and quality and environmental impacts of energy production. *Eur J Agron* 2003;19:45–63. [https://doi.org/10.1016/S1161-0301\(02\)00018-7](https://doi.org/10.1016/S1161-0301(02)00018-7).
- [28] Pude R, Treseler C-H, Trettin R, Noga G. Suitability of *miscanthus* genotypes for lightweight concrete. *Bodenkultur* 2005;56:61–9.
- [29] Kaack K, Schwarz K-U, Brander PE. Variation in morphology, anatomy and chemistry of stems of *Miscanthus* genotypes differing in mechanical properties. *Ind Crop Prod* 2003;17:131–42. [https://doi.org/10.1016/S0926-6690\(02\)00093-6](https://doi.org/10.1016/S0926-6690(02)00093-6).
- [30] Acikel H. The use of *miscanthus* (*Giganteus*) as a plant fiber in concrete production. *Sci Res Essays* 2011;6:2660–7. <https://doi.org/10.5897/SRE10.1139>.
- [31] Dias PP. Dry-stacked insulation masonry blocks based on *miscanthus* concrete. Université du Luxembourg; 2021. <http://hdl.handle.net/10993/47482>.
- [32] Waldmann D, Thapa V, Dahm F, Faltz C. Masonry blocks from lightweight concrete on the basis of *miscanthus* as aggregates. In: Barth S, Murphy-Bokern D, Kalinina O, Taylor G, Jones M, editors. *Perennial biomass crops for a resource-constrained world*. Cham: Springer International Publishing; 2016. p. 273–95. https://doi.org/10.1007/978-3-319-44530-4_23.
- [33] Moll L, Wever C, Völkerling G, Pude R. Increase of *miscanthus* cultivation with new roles in materials production—a review. *Agronomy* 2020;10:308. <https://doi.org/10.3390/agronomy10020308>.
- [34] Khalil N, Aouad G, El Cheikh K, Rémond S. Use of calcium sulfoaluminate cements for setting control of 3D-printing mortars. *Construct Build Mater* 2017;157:382–91. <https://doi.org/10.1016/j.conbuildmat.2017.09.109>.
- [35] Khalil N. Formulation et caractérisation chimique et rhéologique des mortiers imprimables en 3D à base de mélanges de ciments Portland et sulfoalumineux. Université de Lille; 2018. <https://tel.archives-ouvertes.fr/tel-02900865/document>.
- [36] European Committee for Standardization (CEN). NF EN 196-1: methods of testing cement — Part 1: determination of strength. 2016.
- [37] Wu F, Yu Q, Brouwers HJH. Effects of treated *miscanthus* on performance of bio-based cement mortar. *Journal of Sustainable Cement-Based Materials* 2023;12:357–68. <https://doi.org/10.1080/21650373.2022.2059794>.
- [38] AFNOR Editions. NF P18-459. Béton - Essai pour béton durci - Essai de porosité et de masse volumique; 2010.
- [39] European Committee for Standardization (CEN). NF EN ISO 22007-2, Plastics — determination of thermal conductivity and thermal diffusivity — Part 2: transient plane heat source (hot disc) method. 2015.
- [40] Technical specifications of the TPS 2500 S instrument, (n.d.), <https://www.hotdiskinstruments.com/products-services/instruments/tps-2500-s/>.
- [41] Onuaguluchi O, Banthia N. Plant-based natural fibre reinforced cement composites: a review. *Cement Concr Compos* 2016;68:96–108. <https://doi.org/10.1016/j.cemconcomp.2016.02.014>.
- [42] Mansur MA, Aziz MA. A study, of jute fibre reinforced cement composites. *Int J Cem Compos Lightweight Concr* 1982;4:75–82. [https://doi.org/10.1016/0262-5075\(82\)90011-2](https://doi.org/10.1016/0262-5075(82)90011-2).

- [43] Eddhahak-Ouni A, Drissi S, Colin J, Neji J, Care S. Experimental and multi-scale analysis of the thermal properties of Portland cement concretes embedded with microencapsulated Phase Change Materials (PCMs). *Appl Therm Eng* 2014;64:32–9. <https://doi.org/10.1016/j.applthermaleng.2013.11.050>.
- [44] Parameshwaran R, Naresh R, Ram VV, Srinivas PV. Microencapsulated bio-based phase change material-micro concrete composite for thermal energy storage. *J Build Eng* 2021;39:102247. <https://doi.org/10.1016/j.jobbe.2021.102247>.
- [45] Gbekou FK, Benzarti K, Boudenne A, Eddhahak A, Duc M. Mechanical and thermophysical properties of cement mortars including bio-based microencapsulated phase change materials. *Construct Build Mater* 2022;352:129056. <https://doi.org/10.1016/j.conbuildmat.2022.129056>.
- [46] Vogler N, Drabetzki P, Lindemann M, Kühne H-C. Description of the concrete carbonation process with adjusted depth-resolved thermogravimetric analysis. *J Therm Anal Calorim* 2022;147:6167–80. <https://doi.org/10.1007/s10973-021-10966-1>.
- [47] Villain G, Thierry M, Platret G. Measurement methods of carbonation profiles in concrete: thermogravimetry, chemical analysis and gammadensimetry. *Cement Concr Res* 2007;37:1182–92. <https://doi.org/10.1016/j.cemconres.2007.04.015>.
- [48] Yogalakshmi KN, Poornima Devi T, Sivashanmugam P, Kavitha S, Yukesh Kannah R, Varjani S, et al. Lignocellulosic biomass-based pyrolysis: a comprehensive review. *Chemosphere* 2022;286:131824. <https://doi.org/10.1016/j.chemosphere.2021.131824>.
- [49] Berardi U, Gallardo AA. Properties of concretes enhanced with phase change materials for building applications. *Energy Build* 2019;199:402–14. <https://doi.org/10.1016/j.enbuild.2019.07.014>.
- [50] Shafigh P, Asadi I, Akhiani AR, Mahyuddin NB, Hashemi M. Thermal properties of cement mortar with different mix proportions. *Mater Construcción* 2020;70:224. <https://doi.org/10.3989/mc.2020.09219>.
- [51] Pomianowski M, Heiselberg P, Jensen RL. Full-scale investigation of the dynamic heat storage of concrete decks with PCM and enhanced heat transfer surface area. *Energy Build* 2013;59:287–300. <https://doi.org/10.1016/j.enbuild.2012.12.013>.
- [52] Ahmad MR, Chen B, Ali Shah SF. Mechanical and microstructural characterization of bio-concrete prepared with optimized alternative green binders. *Construct Build Mater* 2021;281:122533. <https://doi.org/10.1016/j.conbuildmat.2021.122533>.
- [53] Ntimugura F, Vinai R, Harper A, Walker P. Mechanical, thermal, hygroscopic and acoustic properties of bio-aggregates – lime and alkali - activated insulating composite materials: a review of current status and prospects for miscanthus as an innovative resource in the South West of England. *Sustainable Materials and Technologies* 2020;26:e00211. <https://doi.org/10.1016/j.susmat.2020.e00211>.
- [54] Elfordy S, Lucas F, Tancrét F, Scudeller Y, Goudet L. Mechanical and thermal properties of lime and hemp concrete (“hempcrete”) manufactured by a projection process. *Construct Build Mater* 2008;22:2116–23. <https://doi.org/10.1016/j.conbuildmat.2007.07.016>.
- [55] Schnabel T, Huber H, Petutschnigg A, Jäger A. Analysis of plant materials pre-treated by steam explosion technology for their usability as insulating materials. *Agron Res* 2019;17:1191–8. <https://doi.org/10.15159/AR.19.061>.
- [56] Li G, Yu Y, Zhao Z, Li J, Li C. Properties study of cotton stalk fiber/gypsum composite. *Cement Concr Res* 2003;33:43–6. [https://doi.org/10.1016/S0008-8846\(02\)00915-8](https://doi.org/10.1016/S0008-8846(02)00915-8).